Chemical Engineering Journal 348 (2018) 361–369

Contents lists available at ScienceDirect

Chemical Engineering Journal

journal homepage: www.elsevier.com/locate/cej

Palladium supported on low-surface-area fiber-based materials for catalytic oxidation of volatile organic compounds

Hua Deng[a], Shunyu Kang[a,b], Chunying Wang[a,b], Hong He[a,b,c,*], Changbin Zhang[b,c,*]

[a] Center for Excellence in Regional Atmospheric Environment, Key Laboratory of Urban Pollutant Conversion, Institute of Urban Environment, Chinese Academy of Sciences, Xiamen 361021, China
[b] University of Chinese Academy of Sciences, Beijing 100049, China
[c] Research Center for Eco-Environmental Sciences, Chinese Academy of Sciences, Beijing 100085, China

HIGHLIGHTS

- The noble metal palladium was successfully loaded on low-surface-area fiber materials.
- Pd-Ceramic fiber catalyst is an effective candidate for elimination of VOCs.
- Ceramic fiber was far better than glass fiber owing to high Pd particle dispersion and strong support acidity.

GRAPHICAL ABSTRACT

Pd-Ceramic catalyst is an effective candidate for application to elimination of volatile organic compounds.

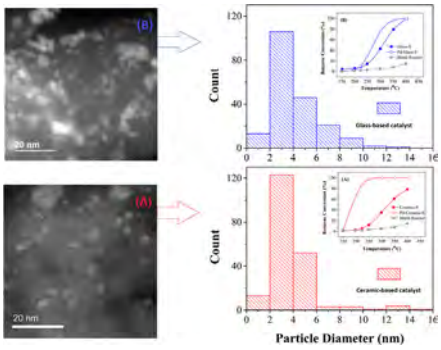

ARTICLE INFO

Keywords:
Volatile organic compound
Catalytic oxidation
Pd based catalyst
Fiber
Benzene

ABSTRACT

Fiber-based palladium catalysts were synthesized via an ultrasonic-assisted impregnation method on ceramic and glass fiber supports pretreated by leaching with water, sulfuric acid and nitric acid, respectively. The as-prepared catalysts were next tested for the catalytic combustion of benzene. The Pd-Ceramic fiber exhibited better activity than Pd-glass fiber in terms of benzene conversion and carbon dioxide yield, and 0.8 wt% Pd loading was the optimum loading amount. The prepared catalysts were characterized by FE-SEM, BET, XRD, XPS, TEM, in situ DRIFTS and TPD. The results indicated that a relatively large surface area, strong support acidity, well-dispersed Pd particles, and suitable redox and desorption properties all contributed to the good performance of ceramic-fiber-based catalysts. Our findings demonstrate that the Pd-Ceramic fiber catalyst is an effective candidate for application in elimination of volatile organic compounds.

1. Introduction

Volatile organic compounds (VOC) are one of the major contributors to air pollution [1–4]. In fact, the progressive increase of VOC emissions not only directly threatens human beings via their potential toxicity, including carcinogenicity, but also indirectly contributes to the formation of photochemical smog and ozone pollution [5–8]. It was reported that China's industrial non-methane VOC emissions increased by a factor of 11.6 from 1980 to 2010 at an average annual rate of 8.5%, increasing to 13.35 Tg in 2010 [9]. With the imposition of

* Corresponding authors at: University of Chinese Academy of Sciences, Beijing 100049, China.
E-mail addresses: hhe@iue.ac.cn, honghe@rcees.ac.cn (H. He), cbzhang@rcees.ac.cn (C. Zhang).

https://doi.org/10.1016/j.cej.2018.04.184
Received 3 January 2018; Received in revised form 23 April 2018; Accepted 26 April 2018
Available online 27 April 2018
1385-8947/

increasingly strict emission regulations, there is more and more demand for post-treatment technologies.

Catalytic oxidation is considered to be one of the most effective ways for reducing VOC emissions due to its low NOx emissions, high destruction efficiency, and low operation and energy costs [1,4]. Among different kinds of catalysts including supported noble metals, transition metal oxides and mixtures of noble metals and metal oxides, the noble metal (Pd and/or Pt) catalysts are recognized as some of the most desirable candidates [10,11]. In particular, the Pd-based catalysts exhibit several desirable practical application features such as low cost, high activity, thermal stability and high tolerance to moisture [12,13]. As a result, Pd-based catalysts have drawn more and more attention from the industry and research community nowadays.

For Pd-based catalysts, the support effect is profound, and their activity has also been found to be closely related to the support type. Usually, Pd-based catalysts have been prepared by loading Pd species on bare or doped Al_2O_3 [14,15], SiO_2, [16] or TiO_2 substrates [17]. Al_2O_3 seems to be one of the most frequently used support components. V [18,19], Mo [20], Nb [21], Cu [22], and Ce [23–25] doped Al_2O_3 supports have been reported to be superior to bare Al_2O_3 for Pd-based catalysts in terms of activity for VOC oxidation, and the support effect has also been intensively examined. Increasing the dispersion of Pd and changing the chemical state of palladium are believed to be the main contributions of the supports. Some porous metal oxides such as hierarchically porous Nb_2O_5 and Ta_2O_5 [26], ordered mesoporous-Co_3O_4 [27,28], 3-dimensionally ordered macroporous Mn_2O_3 etc. [29] have also been recently investigated as effective supports for Pd [29–31]. Molecular sieve supports such as ZSM-5 [32–34], Beta [35], Y [36,37], SBA-15 [38] and so on have been extensively investigated. Moreover, some novel supports like steel wire mesh [39,40], carbon nanofiber [41], glass fiber [42] and pearl shell powder [43] have been also employed to prepare Pd-based catalysts. Among these catalysts, fiber-based supports attract more and more attention as novel materials nowadays [44], since they offer a promising trade-off between mass transfer and pressure drop. Considering their mass and heat transfer, pressure drop, productivity and the possibility to create new types of catalytic reactors, fiber material supported noble metal catalysts are promising candidates for application in elimination of VOCs by catalytic oxidation.

In this work, ceramic and glass fibers were separately used as substrates to support the noble metal Pd, loaded via an ultrasonic-assisted wet impregnation method. Pretreatment methods for the fiber supports by water, sulfuric acid solution and nitric acid solution were compared. The catalytic oxidation of benzene was used as a model reaction [14,15,45] to evaluate all catalysts. The catalysts were also characterized by means of FESEM, BET, XRD, XPS, TEM, in situ DRIFTS and TPD. It was found that ceramic fiber was far better than glass fiber as a support in this study. Well-dispersed Pd particles, strong support acidity, suitable redox and desorption properties all contributed to good performance in elimination of VOC.

2. Materials and methods

2.1. Experimental section

To remove the impurities from the fiber substrates and enhance the metal-support interaction, sulfuric acid and nitric acid were used to leach the fiber supports firstly. A certain amount of ceramic fiber (Triton Kaowool) or glass fiber (ACROS glass wool) was immersed in 50% H_2SO_4 or HNO_3 for 30 min each time and 3 times in all, then washed with deionized water until the washes were neutral and subsequently dried (denoted as Ceramic-S, Ceramic-N, Glass-S and Glass-N respectively). For comparison, deionized water was also used to leach both fiber supports (denoted as Ceramic-W or Glass-W). The Pd/fiber catalysts with different palladium loadings (0.4, 0.8, and 1.2 wt%) were prepared by an impregnation method. The Pd loading was calibrated and confirmed by ICP-OES measurements. An appropriate amount of the resulting ceramic fiber or glass fiber was immersed into an aqueous solution of palladium nitrate ($Pd(NO_3)_2$). After ultrasonic-assisted impregnation for 1 h, the excess water was removed by a rotary evaporator under vacuum at 60 °C. Then the sample was calcined in a furnace at 500 °C for 3 h. The final samples were named in the form of Pd-fiber precursor-leaching solution. For example, the sample denoted as Pd-Ceramic-S means Pd was loaded on the ceramic fiber support and the fiber precursor was leached with H_2SO_4 before loading. Except where otherwise stated, the palladium load is 0.8 wt% on the support in all cases. For comparison, the same impregnation procedures were followed for the pure supports. Before activity tests and characterization, all samples were reduced with H_2 at 300 °C for 1 h.

2.2. Catalytic measurements

A gaseous mixture of C_6H_6 (1500 ppm), water vapor (2%, when used), and O_2 (20%) in N_2 balance at a volumetric flow rate of 300 mL min^{-1} was fed into a laboratory-built fixed-bed reactor. The catalytic activity was measured in the instrument, where fiber-based catalyst with weight of 0.2 g was packed in the bed (GHSV = 90,000 mL h^{-1} g^{-1}). The benzene concentration was analyzed online by a gas chromatograph (GC; Agilent 7890B, HP-5 capillary column) with a flame ionization detector. CO_2 and O_2 concentrations were analyzed by the same GC equipped with a thermal conductivity detector (Porapak Q and HayeSep Q columns). In all the experiments, C_6H_6 conversion was calculated using the following equation:

$$C_6H_6\ Conversion\ (\%) = \left(1 - \frac{[C_6H_6]_{out}}{[C_6H_6]_{in}}\right) \times 100\%$$

The CO_2 yield was defined as follows:

$$CO_2\ Yield\ (\%) = \frac{[CO_2]_{out}}{[C_6H_6]_{in} \times 6} \times 100\%$$

2.3. Catalyst characterization

The X-ray powder diffraction patterns of the various catalysts were collected on a wide angle X'Pert Pro XRD diffractometer (PANalytical B.V., Netherlands), using CuKα radiation (λ = 1.5406 Å) at 40 kV and 40 mA with a scanning speed of 5°/min. The patterns were taken over the 2θ range from 10° to 90°.

The morphology of catalysts was imaged using a Hitachi S-4800 scanning electronic microscope (Hitachi, Japan). The samples for FE-SEM measurements were prepared by depositing the powder on a conductive tape using N_2 vertical purging. The voltage employed for lower amplification was 3 kV while for higher amplification it was 1 kV. The catalyst samples were sputter-coated with platinum prior to imaging. High-angle annular dark-field scanning transmission electron microscopy (HAADF-STEM) was performed on a JEOL JEM-ARM2100F TEM with Cs-corrected probe operated at 200 kV.

Nitrogen adsorption-desorption isotherms were measured using a Quantachrome QuadraSorb evo system at 77 K. The specific surface area of the samples was calculated by the Brunauer-Emmett-Teller (BET) method. The volume of pores was determined by the Barrett-Joyner-Halenda (BJH) method from the desorption branches of the isotherms.

X-ray photoelectron spectroscopy (XPS) measurements were carried out with an ESCALAB250 spectrometer using a monochromated Al Kα X-ray source (1486.6 eV). The binding energy was calibrated using the adventitious C 1s peak at 284.6 eV. The continuum spectrum was fitted according to Gaussian-Lorentzian line shapes.

In situ DRIFTS spectra were recorded on a Thermo Fisher is50 FT-IR spectrometer, equipped with an in situ diffuse reflectance chamber

(Harrick) and a high sensitivity MCT/A detector. All fiber catalysts were finely ground and placed in ceramic crucibles in the in situ chamber. Prior to recording each DRIFTS spectrum, the sample was heated in situ in N_2 flow at 573 K for 1 h, then cooled to the desired temperature to measure a reference spectrum. All spectra were measured with a resolution of 4 cm^{-1} and with an accumulation of 32 scans.

The temperature-programmed desorption of CO (CO-TPD) measurements on the samples were carried out on a laboratory-built fixed-bed instrument with a temperature-programmed furnace. The catalysts were loaded in a quartz reactor and heated at 300 °C for 1 h in 100 mL min^{-1} He flow. After being cooled to ambient temperature, the samples were saturated by 1 vol% CO/He mixed gas for 1 h. Then the flow gas was changed to pure He for 0.5 h, followed by temperature ramping to 500 °C at a linear rate of 10 °C min^{-1}. The products CO and CO_2 were monitored using an Ametek LC-D200M PRO Mass Spectrometer at *m/z* ratios of 4, 28 and 44, respectively.

The temperature-programmed desorption of C_6H_6 (C_6H_6-TPD) measurements on the samples were carried out on a laboratory-built fixed-bed instrument with a temperature-programmed furnace. The catalysts were loaded in a quartz reactor and heated at 300 °C for 2 h in 5 vol% H_2 + N_2 flow. The absorbed CO_2 and H_2O was removed and the catalyst was activated at the same time. After being cooled to ambient temperature, the samples were saturated by C_6H_6 nitrogen mixed gas for 1 h. Then the flow gas was changed to pure nitrogen for 0.5 h, followed by temperature ramping to 400 °C at a linear rate of 10 °C min^{-1}. The products C_6H_6, H_2O, H_2 and CO_2 were monitored using an Ametek LC-D200M PRO Mass Spectrometer at *m/z* ratios of 78, 18, 2 and 44, respectively.

3. Results and discussion

3.1. Catalytic activity of fiber-based catalysts

The conversion of C_6H_6 over different fiber-based catalysts is displayed in Fig. 1. It can be clearly seen in Fig. 1(A) that the Pd-Ceramic fiber catalysts exhibited good performance in eliminating volatile benzene. The complete conversion temperature was about 250 °C. When the ceramic fiber support was leached with H_2SO_4 or HNO_3, the conversion of C_6H_6 over the whole range was improved slightly, and H_2SO_4 was the best leaching solution. Pretreating the ceramic fiber by leaching with water or acid probably does not result in remarkable differences in the redox properties. That is the reason why Pd-Ceramic-W, Pd-Ceramic-S, and Pd-Ceramic-N exhibited similar benzene oxidation conversion profiles. As for the glass fiber catalysts shown in Fig. 1(B), the C_6H_6 conversion was far lower than that of the ceramic-based catalysts. For instance, only 30% conversion could be obtained at the same reaction temperature of 250 °C. Leaching with H_2SO_4 could improve the activity.

It is well known that noble metals such as Pd, Pt, Ir are the active components in catalytic combustion of VOC [10]. As clearly shown in Fig. 1(C), the bare Glass-S was better than Ceramic-S in catalytic combustion of benzene. Loading with Pd significantly enhanced the catalytic performance for both fiber supports. The general conversion order for all samples can be described as Pd-Ceramic-S > Pd-Glass-S > Glass-S > Ceramic-S > Blank Reactor. Pd and the ceramic fiber support are a suitable match to form the best catalyst in this study. A summary of benzene oxidation over Pd-based catalysts is listed in Table 1. Our catalysts exhibited outstanding combined performance in terms of catalytic efficiency and GHSV value among the class of supported monometallic Pd-based catalysts. It is worth noting from the table that our usage amount of noble metal Pd is slightly higher than for the zeolite support catalysts [32,38]. The mixing with transition metal

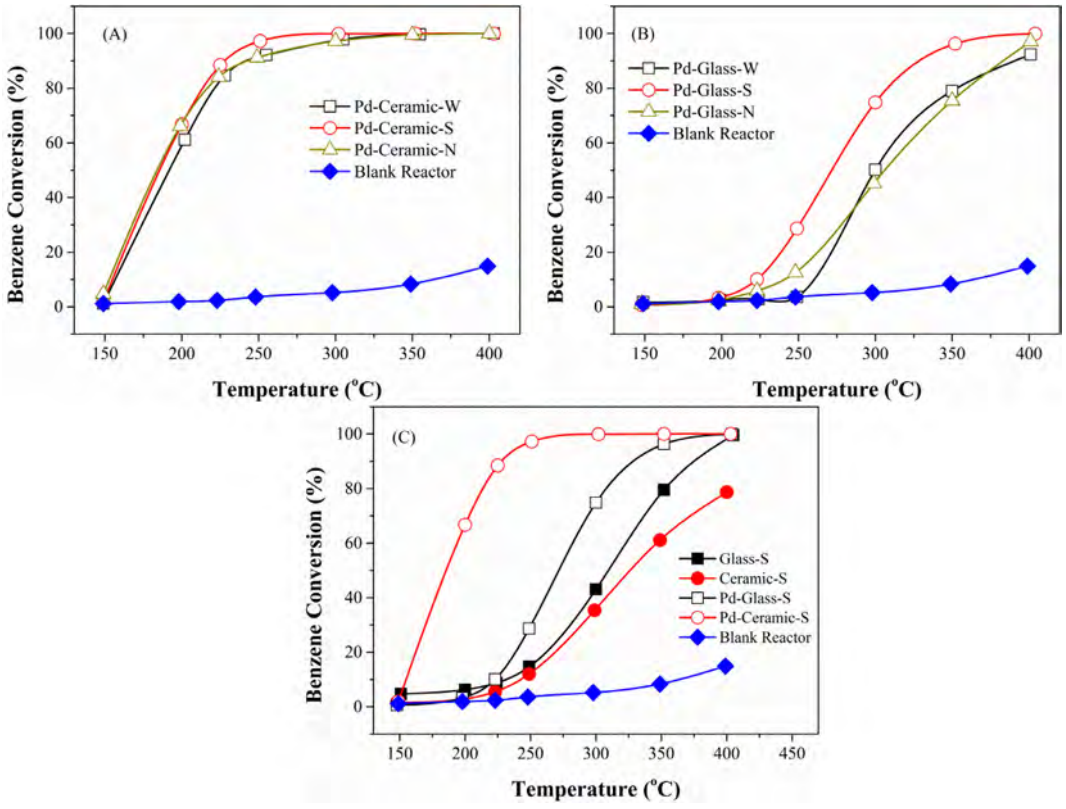

Fig. 1. (A) C_6H_6 conversion over 0.8 wt% ceramic-based catalysts (B) C_6H_6 conversion over 0.8 wt% glass-based catalysts (C) Comparison of the C_6H_6 conversion over different fiber-based catalysts.

Table 1
Summary of benzene oxidation catalysts that are known to exhibit good performance.

Catalyst	Weight (g)	Benzene Concentration (ppm)	Flow (mL/min)	GHSV (mL g^{-1} h^{-1})	T_{90} (°C)	Refs.
1 wt% Pd/Al_2O_3	0.2	1000	100	30,000	270	[15]
1 wt% Pd/γ-Al_2O_3	0.6	1000	52.5	5250	250	[14]
0.2 wt% Pd/6 wt% Ce/pearl shell	0.375 mL	1000	125	20,000 h^{-1}	290	[43]
0.2 wt% Pd/10 wt% Ni/SBA-15	0.05	1000	100	120,000	258	[38]
0.3 wt%Pd/ZSM-5/MCM-48	0.3	1500	350	70,000	209	[34]
0.2 wt% Pd/6 wt% La-ZSM-5-OM	0.375 mL	1000	125	20,000 h^{-1}	250	[32]
1.5 wt% Pd/SiO_2	0.1	2550	-	800 h^{-1}	197	[16]
0.8 wt% Pd/10 wt% V_2O_5/Al_2O_3	0.06	482	30	30,000	270	[19]
0.8 wt% Pd-Ceramic-S	0.2	1500	300	90,000 (34,000 h^{-1})	225	This study
0.8 wt% Pd-Glass-S	0.2	1500	300	90,000 (34,000 h^{-1})	330	

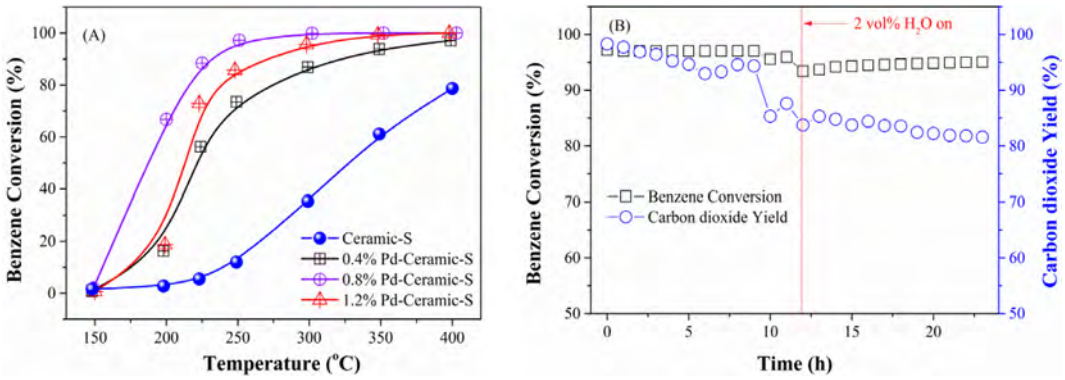

Fig. 2. (A) C_6H_6 conversion over ceramic-based catalysts with different palladium loadings (B) Stability test of Pd-Ceramic-S catalyst in terms of C_6H_6 conversion and CO_2 yield at temperature of 250 °C.

oxides like La, Ni on ZSM-5 [32] or SBA-15 [38] supports respectively is believed to partially play the role of palladium in combustion of VOC.

The Pd loading effect on ceramic fiber was also examined and plotted in Fig. 2(A). Increasing the Pd content from 0 to 0.8 wt% significantly enhanced the C_6H_6 conversion: the sample with 0.8 wt% Pd exhibited the highest C_6H_6 conversion, and the light-off temperature for above 90% conversion was reduced to 225 °C. Further increasing the Pd content to 1.2 wt% significantly decreased the C_6H_6 conversion, indicating that there is an optimal amount of noble metal that can be dispersed on the ceramic fiber. The selected 0.8 w% Pd-Ceramic-S catalyst was also evaluated by stability testing. It is clearly shown in Fig. 2(B) that the catalyst exhibited excellent stability, maintaining above 97% C_6H_6 conversion and 94% CO_2 yield at the temperature of 250 °C for a 12 h test. Adding 2 vol% H_2O into the gas feed, the C_6H_6 conversion and CO_2 yield were depressed to certain extents. The catalyst could also maintain above 93% C_6H_6 conversion and 82% CO_2 yield throughout another 12 h test. This result agrees with other reports [4] that H_2O in the reaction mix only slightly affects the C_6H_6 conversion performance, but significantly restrains the CO_2 yield. The stability of lower benzene conversion at the temperature of 200 °C was also tested, with results shown in Fig. S1 and by-product measurement by on-line mass spectra is illustrated in Fig. S2.

3.2. Structural properties

In order to learn the key factors that lead to the differences in activity between the two types of fiber-supported catalysts, the Pd-based fiber catalysts were characterized by FE-SEM, XRD, and BET measurements. FE-SEM images of the ceramic and glass fiber catalyst samples are shown in Fig. 3. The ceramic fiber catalysts are composed of non-uniformly bent rods with diameter of about 5 μm (as shown in Fig. 3A and B). After Pd loading, the surface of the ceramic was no longer smooth. On the other hand, the glass fiber catalysts are composed of uniform straight rods with diameter of about 10 μm and length of about 500 μm. Like the case with the ceramic fiber catalyst, noble metal loading led to the surface of the fiber support becoming rough, while the overall morphology for both fiber materials was unchanged after noble metal loading. Based on these results, we can tentatively presume that the catalyst surface area increased after loading, which is considered to be beneficial for benzene combustion.

As shown in Table 2, the pure ceramic and glass fibers were dominated by their external surface, which exhibited extremely low BET surface areas of 0.09 and 0.12 m^2/g respectively (isotherms are shown in Fig. S3). This is reasonable because fiber materials usually do not demonstrate advanced porous structures [42]. On the other side of the coin, fiber offers a promising trade-off between mass transfer and pressure drop [44]. Neither water nor sulfuric acid leaching of the pure fiber supports increased the surface area. However, loading palladium onto the surface resulted in a significant increase in surface area, which was accompanied by an increase in pore volume. It is worth noting that the textural parameters of the ceramic fiber catalysts increased about 10-fold after noble metal loading, while a 5-fold increase was observed for the glass fiber materials. The pore distribution results also agree with this conclusion. As shown in Fig. 4, palladium loading significantly enhanced the pore volume in the diameter range of 3–10 nm. The pore volume increase was more profound for the ceramic-based catalyst than the glass fiber material. This indicated that pore-creation occurred more easily on ceramic fiber than glass fiber. Presumably, palladium has a strong interaction with the ceramic fiber.

All samples were also characterized by XRD measurements (Fig. S4). The fiber supports and catalysts exhibited a mostly amorphous structure, although the SiO_2 phase could be discerned in both fiber-based catalysts. In all cases, no metallic Pd or PdO phase could be observed. This suggests that the c surface of both types of fiber supports.

3.3. The chemical state and particle distribution of Pd species

The chemical states of supported Pd were characterized by XPS,

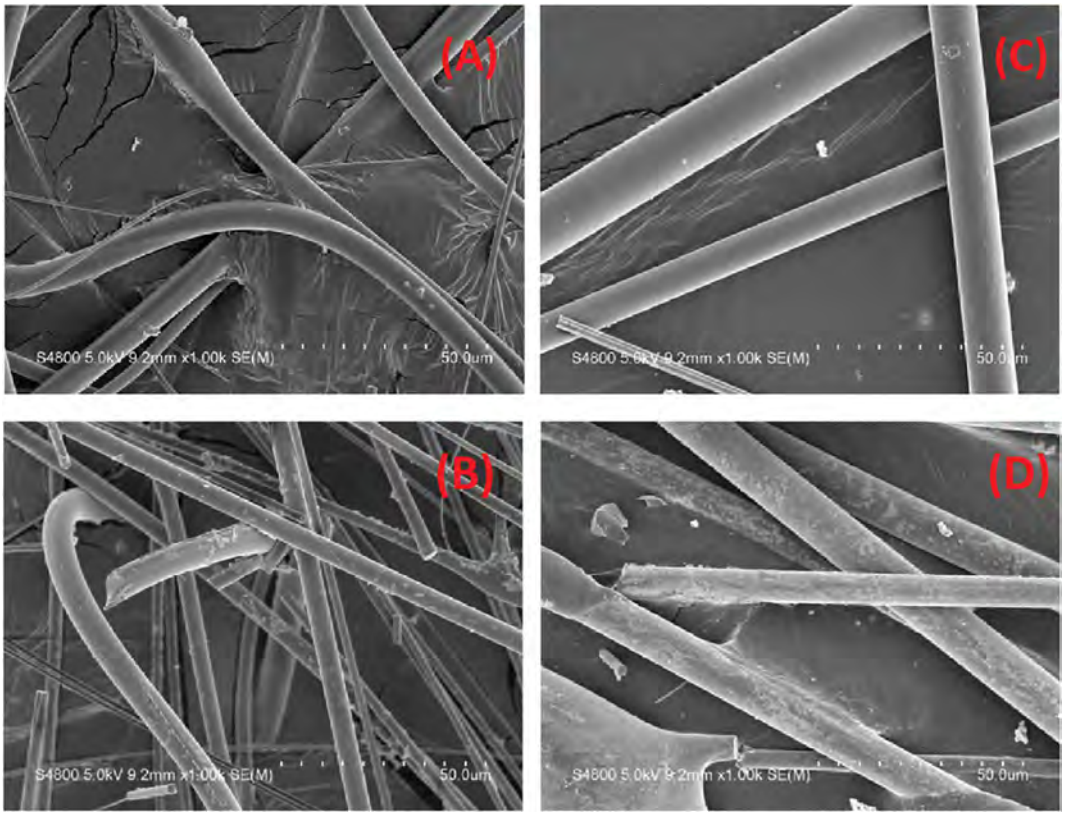

Fig. 3. SEM images of the fiber-based catalysts, (A) Ceramic-S, (B) Pd-Ceramic-S, (C) Glass-S, (D) Pd-Glass-S.

Table 2
Textural parameters of fiber-based catalysts derived from N_2 physisorption and Pd^{2+}/Pd^0 ratio from XPS results.

sample	BET (m^2/g)	Pore volume ($\times 10^{-4}$ cc/g)	Pd^{2+}/Pd^0
Ceramic-W	0.09	1.72	
Glass-W	0.12	4.71	
Ceramic-S	0.08	1.46	
Glass-S	0.13	4.71	
Pd-Ceramic-W	2.01	17.96	0.63
Pd-Glass-W	0.89	17.57	1.49
Pd-Ceramic-S	1.14	12.59	2.00
Pd-Glass-S	0.61	20.33	3.66

with the results shown in Fig. 5. The Pd $3d_{5/2}$ binding energy peaks for all samples appeared at around 334.4–336.7 eV, which is consistent with the values reported in previous studies [14,15,27,32,34,38].

Two kinds of Pd species were observed on both Pd-Ceramic-S and Pd-Glass-S catalysts after deconvolution of the XPS peaks. The peaks located at 335.9 and 335.6 eV for Pd-Glass-S and Pd-Ceramic-S respectively can both be assigned to Pd^{2+}/PdO [46]. The peak at 334.4 eV on the Pd-Glass-S catalyst and 334.7 eV on the Pd-Ceramic-S catalyst can be ascribed to metallic Pd/Pd^0 [46]. The Pd^{2+} to Pd^0 ratios are listed in Table 2. Different catalysts exhibited quite different ratios of Pd^{2+} to Pd^0. No obvious relationship between the ratio and catalytic activity could be found in this study, thus C_6H_6 decomposition seems to not be exclusively affected by the ratio of Pd^{2+} to Pd^0. In other words, both Pd^{2+} and Pd^0 are responsible for the oxidation of benzene, which is supported by other works [14,15,34]. The Mars-van Krevelen mechanism is usually applied to hydrocarbon oxidation over Pd-based catalysts [34,47]. The support acidity is crucial [48,49], since acidic supports have stronger electrophilic character, which can accelerate the transformation from Pd^0 to Pd^{2+} more easily and finally promote the catalytic process. The NH_3-TPD results for both fiber supports are displayed in Fig. S5. The total acidity of the ceramic fiber

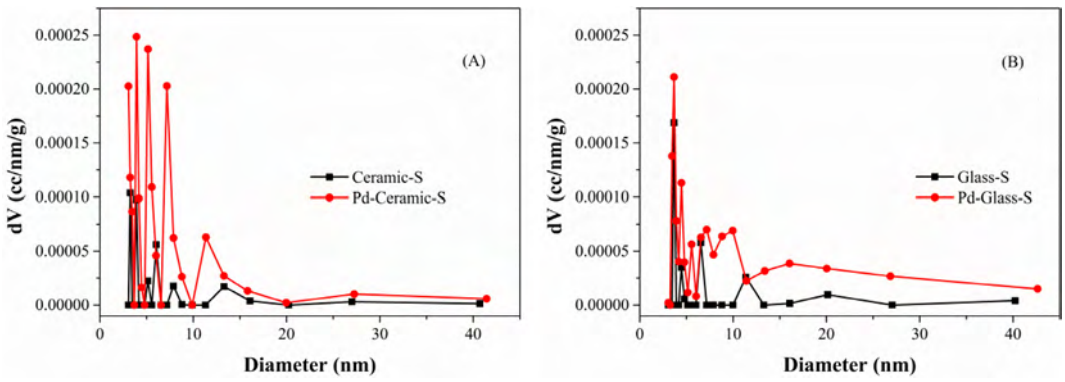

Fig. 4. Comparison of pore distribution for fiber support and palladium fiber-based catalysts: (A) Ceramic fiber, (B) Glass fiber.

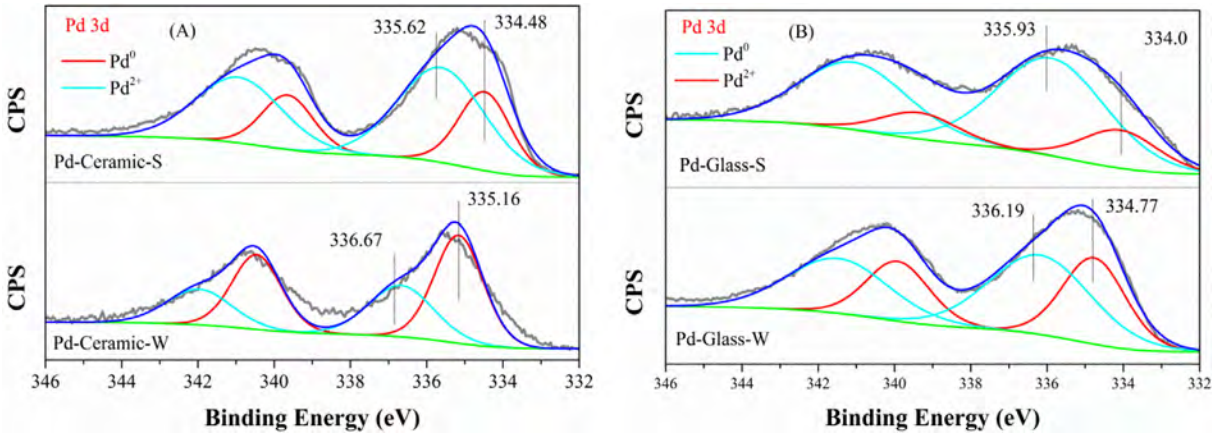

Fig. 5. XPS spectra of Pd 3d level for Pd fiber-based catalysts (A) Ceramic fiber, (B) Glass fiber.

(37.76 μmol g^{-1}) is significantly higher than that of glass fiber (29.05 μmol g^{-1}) and the main desorption temperature of ceramic fiber (530 °C) is higher than that of glass fiber (330 °C), confirming that the ceramic support is more acidic than the glass support in terms of acid site density and strength. It is therefore reasonable that Pd supported on ceramic fiber performs better in benzene oxidation than that on glass fiber.

In order to confirm the Pd species distribution on the fiber support, HAADF/STEM experiments were conducted, and the results are displayed in Fig. S6. It is clear that Pd species are more highly dispersed on ceramic fiber than on glass fiber. The average nano-particle size for Pd-Ceramic-S is 3.89 nm, while that for Pd-Glass-S is 4.25 nm, as shown in Fig. 6. It has been reported that the average Pd particle size is about 7–14 nm on Al_2O_3 supports [14,15], and H_2 reduction can increase the Pd particle size to 12–17 nm [14,15]. Our result is much smaller than that and close to the particle size found for Pd supported on ZSM-5/MCM-48 zeolite, with diameter of 3.07 nm [34]. Herein, all results led us to conclude that the ceramic fiber may have a favorable mutual interaction with the noble metal Pd, which improves the dispersion of Pd atoms on the surface and finally promotes the catalytic efficiency.

3.4. Surface mechanism

The catalytic combustion of VOC usually starts with the adsorption of organic compounds, thus in situ DRIFTS spectra were collected first for a 300 mL min^{-1} flow of C_6H_6 (1500 ppm) and N_2 balance over the catalyst at a fixed temperature of 250 °C. After attaining the adsorption steady state, 20 vol% O_2 was introduced into the flow to oxidize the adsorbed species on the surface of catalyst. Finally, C_6H_6 was removed from the flow to observe the desorption properties of adsorbed species on the surface. For ease of comparison, the steady state spectra obtained under three different reaction conditions for both Pd-fiber catalysts are

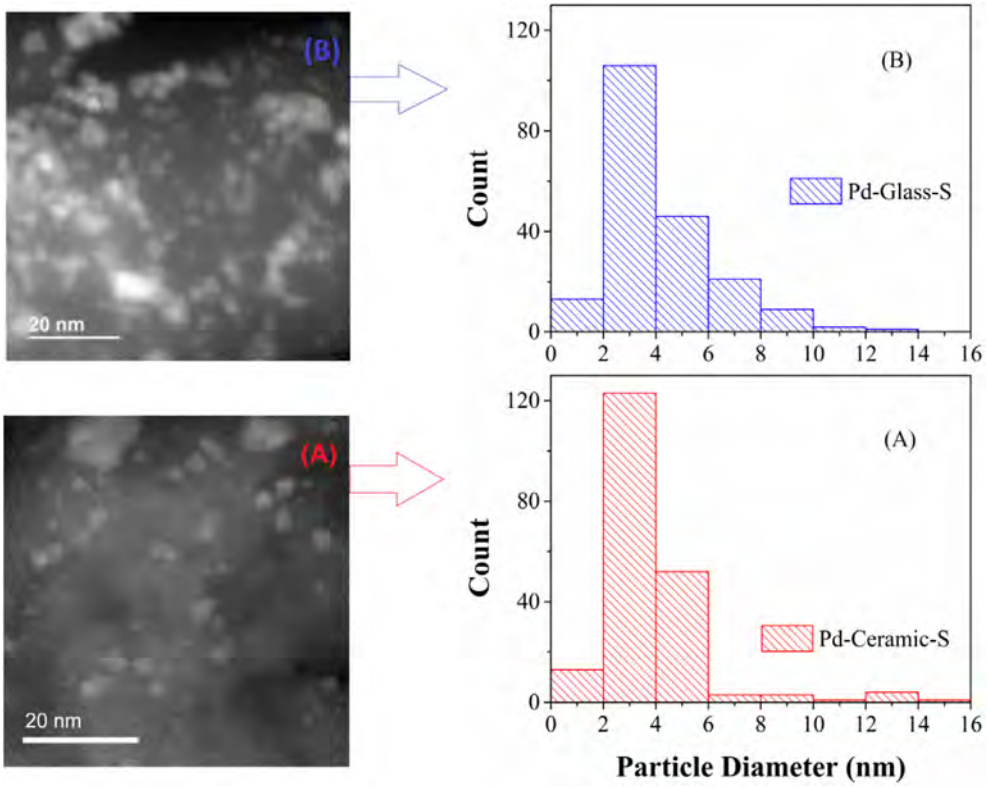

Fig. 6. The particle distribution of Pd-fiber-based catalysts (A) Pd-Ceramic-S, (B) Pd-Glass-S.

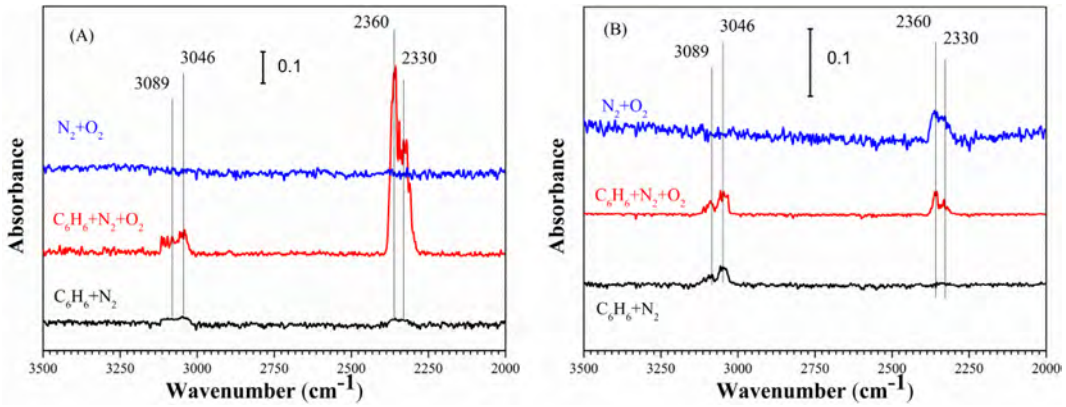

Fig. 7. In situ DRIFTS spectra of adsorbed species on fiber-based catalysts at different steady state at temperature of 250 °C (A) Pd-Ceramic-S, (B) Pd-Glass-S.

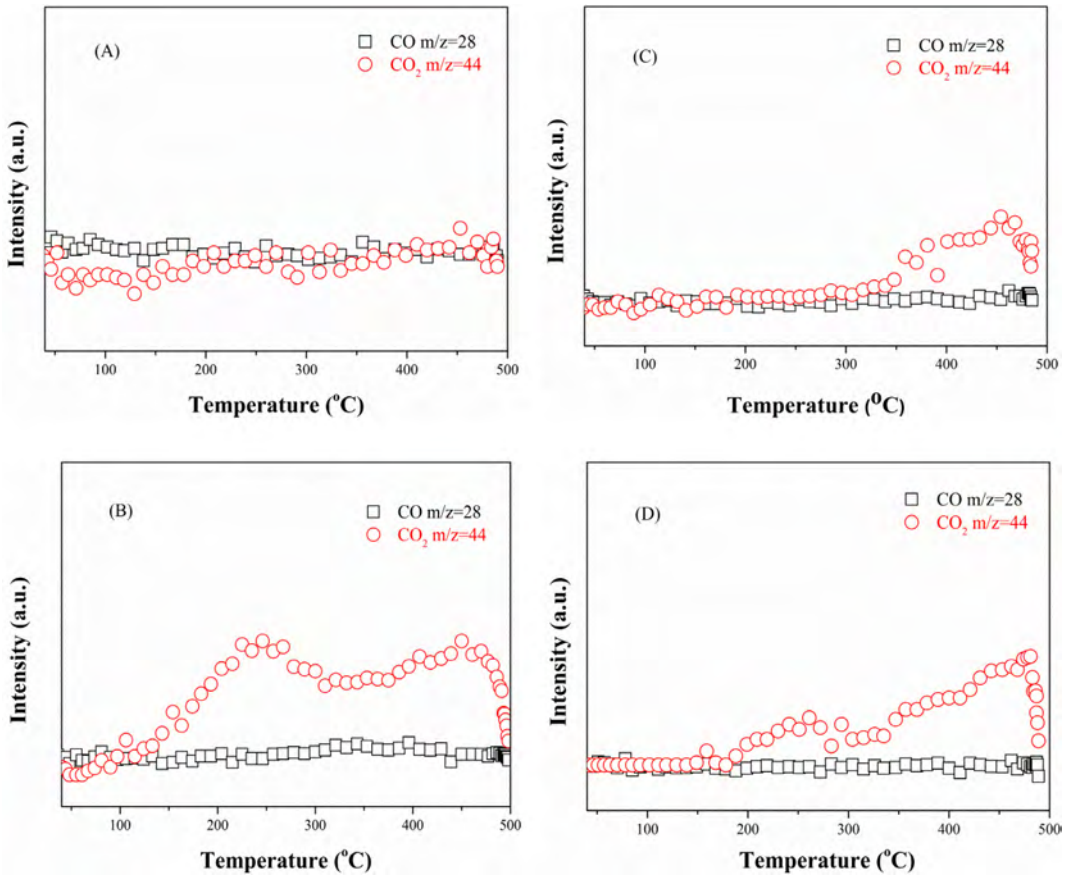

Fig. 8. CO-TPD profiles of fiber-based catalyst, (A) Ceramic-S, (B) Pd-Ceramic-S, (C) Glass-S and (D) Pd-Glass-S.

plotted in Fig. 7.

As shown in Fig. 7, exposure of different catalysts to the feed gas of $C_6H_6 + N_2$ resulted in the appearance of four peaks (3089, 3046, 2360, 2330 cm^{-1}) within the range of 3500–2000 cm^{-1}. In accordance with other reports [50,51], the peaks at 3089 and 3046 were assigned to the stretching C—H deformation vibration of adsorbed benzene species, which is close to the values observed for gaseous benzene (3038–3057 cm^{-1}). Peaks at 2360 and 2330 cm^{-1} were due to carbonate species (ad CO_3^{2-}) adsorbed on the catalyst surface [52]. Introducing benzene onto Pd-Ceramic-S and Pd-Glass-S not only produced adsorbed benzene species but also generated a small amount of carbonate species. Adding O_2 to the flow resulted in a significant increase of carbonate species on Pd-Ceramic-S and slight growth on Pd-Glass-S. After removing C_6H_6 from the flow, carbonate species could be completely consumed on Pd-Ceramic-S but still remained on Pd-Glass-S. All the results are consistent with the activity tests (as shown in Fig. 1), showing that Pd-Ceramic-S is more active than Pd-Glass-S in oxidizing benzene.

To confirm the activity of surface oxygen species and desorption properties of C_6H_6 on the fiber-based catalysts, CO-TPD and C_6H_6-TPD was carried out next. As shown in Fig. 8, CO_2 is produced by the surface reaction between the adsorbed CO and the oxygen species of fiber-based catalysts. A CO_2 desorption peak can be detected at a temperature of 400 °C over pure glass fiber but not ceramic fiber, as shown in Fig. 8(A) and (C), indicating that pure glass fiber is more active that ceramic fiber, and the result is consistent with the benzene oxidation performance as shown in Fig. 1(C). After Pd loading on ceramic or glass fiber, both samples exhibited a remarkable CO_2 desorption peak, as

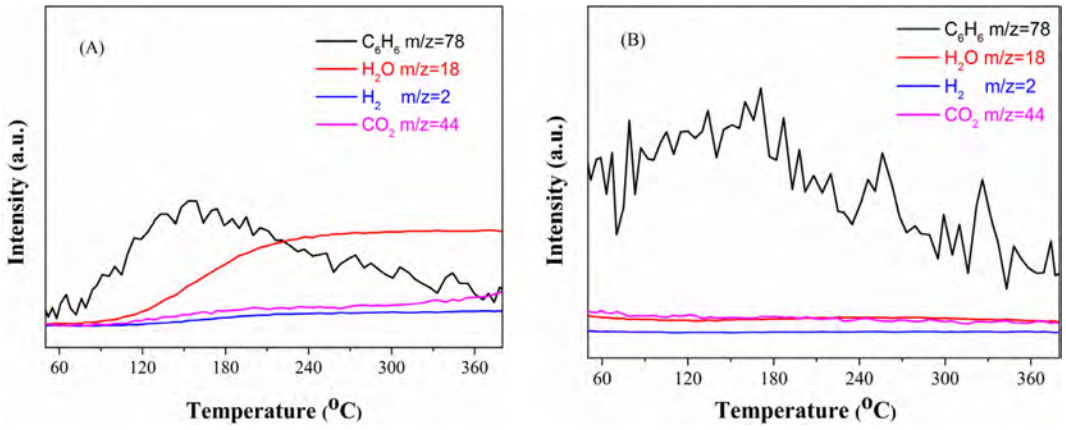

Fig. 9. C_6H_6-TPD results of fiber-based catalysts, (A) Pd-Ceramic-S, (B) Pd-Glass-S.

shown in Fig. 8(B) and (D). The main desorption peak of CO_2 derived from Pd-Glass-S increases marginally but does not move toward lower temperature significantly. However, the corresponding peak of Pd-Ceramic-S is centered at the lower temperature of 250 °C. Thus, the surface oxygen species on Pd-Ceramic-S is more active than that on Pd-Glass-S, and the noble metal Pd probably interacts more favorably with ceramic rather than glass fiber.

The C_6H_6-TPD results are presented in Fig. 9, showing that the C_6H_6 molecules started to desorb at around 120 °C and reached their peak at about 160 °C on both Pd-Ceramic-S and Pd-Glass-S catalysts. The main difference between these catalysts is that the by-products CO_2, H_2O, and H_2 can be detected for Pd-Ceramic-S during ramping of temperature, which indicated that Pd-Ceramic-S can oxidize adsorbed C_6H_6 to CO_2 via its surface oxygen species. This is consistent with the DRIFTS and CO-TPD results, showing that Pd-Ceramic-S exhibits much better redox properties and more active surface oxygen species than those of Pd-Glass-S.

In summary, Pd loading led to a significant increase in surface area and pore volume on the ceramic-based catalyst via pore-creation. STEM results demonstrated that higher Pd dispersion was obtained on ceramic fiber than on glass fiber. Higher Pd dispersion may play a key role in benzene oxidation since well-dispersed small size Pd particles can provide more active sites to activate and dissociate O_2. [14,15,28,34,46,53] The acid/base properties of the support can control the dispersion and the oxidation state of noble metals. The acid properties of supports are considered to be crucial for preparation of catalysts with high Pd dispersion. [54–57] Okumura et al [48,49] and He et al [34] have demonstrated that an acidic support with electrophilic character results in electron-deficient Pd species at the interface. The transformation of Pd^0 to Pd^{2+} may accelerate due to the acidity of the support, which can promote the catalytic oxidation of VOC. [34,48] The NH_3-TPD results suggest that the ceramic support is more acidic than the glass support. Thus, the Pd-Ceramic interface should be more active than Pd-glass in benzene oxidation. In addition, DRIFTS, CO-TPD and C_6H_6-TPD experiments indicated that the mobility and activity of surface oxygen species derived from ceramic fiber are better than those of glass fiber. Herein, we can conclude that the ceramic fiber has a favorable mutual interaction with the noble metal Pd. All results are consistent and demonstrate that the Pd-Ceramic fiber catalyst is an effective candidate for application in the elimination of VOC.

4. Conclusions

The noble metal palladium was successfully loaded on ceramic and glass fiber substrates respectively via an ultrasonic-assisted impregnation method. Leaching the fiber support with sulfuric acid solution prior to Pd loading was beneficial for the benzene combustion performance. Ceramic was better than glass fiber as a noble metal support, and 0.8 wt % Pd loading was the optimum loading amount. BET, XRD, TEM, DRIFTS and TPD results indicated that the ceramic fiber-based catalyst had relatively larger surface area, higher Pd particle dispersion, stronger support acidity, more active surface oxygen species, and favorable mutual metal and support interaction, all of which contribute to its superior performance in the VOC catalytic combustion process.

Acknowledgements

The work was supported by the National Key R&D Program of China (2017YFC0211802) and the National Natural Science Foundation of China (51608504).

Appendix A. Supplementary data

Supplementary data associated with this article can be found, in the online version, at http://dx.doi.org/10.1016/j.cej.2018.04.184.

References

[1] M.S. Kamal, S.A. Razzak, M.M. Hossain, Catalytic oxidation of volatile organic compounds (VOCs) – a review, Atmos. Environ. 140 (2016) 117–134.
[2] F.Y. Hu, J.J. Chen, Y. Peng, H. Song, K.Z. Li, J.H. Li, Novel nanowire self-assembled hierarchical CeO_2 microspheres for low temperature toluene catalytic combustion, Chem. Eng. J. 331 (2018) 425–434.
[3] J. Ji, Y. Xu, H.B. Huang, M. He, S.L. Liu, G.Y. Liu, R.J. Xie, Q.Y. Feng, Y.J. Shu, Y.J. Zhan, R.M. Fang, X.G. Ye, D.Y.C. Leung, Mesoporous TiO_2 under VUV irradiation: enhanced photocatalytic oxidation for VOCs degradation at room temperature, Chem. Eng. J. 327 (2017) 490–499.
[4] J. Chen, X. Chen, W.J. Xu, Z. Xu, J.Z. Chen, H.P. Jia, J. Chen, Hydrolysis driving redox reaction to synthesize Mn-Fe binary oxides as highly active catalysts for the removal of toluene, Chem. Eng. J. 330 (2017) 281–293.
[5] B.L. Wang, Y. Liu, M. Shao, S.H. Lu, M. Wang, B. Yuan, Z.H. Gong, L.Y. He, L.M. Zeng, M. Hu, Y.H. Zhang, The contributions of biomass burning to primary and secondary organics: a case study in Pearl River Delta (PRD), China, Sci. Total Environ. 569 (2016) 548–556.
[6] H.F. Zhang, J. Hu, Y.X. Qi, C.L. Li, J.M. Chen, X.M. Wang, J.W. He, S.X. Wang, J.M. Hao, L.L. Zhang, L.J. Zhang, Y.X. Zhang, R.K. Li, S.L. Wang, F.H. Chai, Emission characterization, environmental impact, and control measure of PM2.5 emitted from agricultural crop residue burning in China, J. Clean. Prod. 149 (2017) 629–635.
[7] W.J. Wu, B. Zhao, S.X. Wang, J.M. Hao, Ozone and secondary organic aerosol formation potential from anthropogenic volatile organic compounds emissions in China, J. Environ. Sci.-China 53 (2017) 224–237.
[8] S.J. Guo, J.H. Tan, J.C. Duan, Y.L. Ma, F.M. Yang, K.B. He, J.M. Hao, Characteristics of atmospheric non-methane hydrocarbons during haze episode in Beijing, China, Environ. Monit. Assess. 184 (2012) 7235–7246.
[9] K.Q. Qiu, L.X. Yang, J.M. Lin, P.T. Wang, Y. Yang, D.Q. Ye, L.M. Wang, Historical industrial emissions of non-methane volatile organic compounds in China for the period of 1980–2010, Atmos. Environ. 86 (2014) 102–112.
[10] L.F. Liotta, Catalytic oxidation of volatile organic compounds on supported noble metals, Appl. Catal. B-Environ. 100 (2010) 403–412.
[11] S. Ojala, S. Pitkaaho, T. Laitinen, N.N. Koivikko, R. Brahmi, J. Gaalova, L. Matejova, A. Kucherov, S. Paivarinta, C. Hirschmann, T. Nevanpera, M. Riihimaki, M. Pirila, R.L. Keiski, Catalysis in VOC abatement, Top. Catal. 54 (2011) 1224–1256.
[12] T. Garcia, B. Solsona, D. Cazorla-Amoros, A. Linares-Solano, S.H. Taylor, Total

oxidation of volatile organic compounds by vanadium promoted palladium-titania catalysts: comparison of aromatic and polyaromatic compounds, Appl. Catal. B-Environ. 62 (2006) 66–76.
[13] T. Garcia, B. Solsona, D.M. Murphy, K.L. Antcliff, S.H. Taylor, Deep oxidation of light alkanes over titania-supported palladium/vanadium catalysts, J. Catal. 229 (2005) 1–11.
[14] J. Liu, H.M. Wang, Y. Chen, M.D. Yang, Y.L. Wu, Effects of pretreatment atmospheres on the catalytic performance of Pd/gamma-Al_2O_3 catalyst in benzene degradation, Catal. Commun. 46 (2014) 11–16.
[15] S.C. Kim, W.G. Shim, Properties and performance of Pd based catalysts for catalytic oxidation of volatile organic compounds, Appl. Catal. B-Environ. 92 (2009) 429–436.
[16] S. Lambert, C. Cellier, E.M. Gaigneaux, J.P. Pirard, B. Heinrichs, Ag/SiO_2, Cu/SiO_2 and Pd/SiO_2 cogelled xerogel catalysts for benzene combustion: relationships between operating synthesis variables and catalytic activity, Catal. Commun. 8 (2007) 1244–1248.
[17] T. Barakat, V. Idakiev, R. Cousin, G.S. Shao, Z.Y. Yuan, T. Tabakova, S. Siffert, Total oxidation of toluene over noble metal based Ce, Fe and Ni doped titanium oxides, Appl. Catal. B-Environ. 146 (2014) 138–146.
[18] S. Pitkaaho, L. Matejova, K. Jiratova, S. Ojala, R.L. Keiski, Oxidation of perchloroethylene-activity and selectivity of Pt, Pd, Rh, and V_2O_5 catalysts supported on Al_2O_3, Al_2O_3-TiO_2 and Al_2O_3-CeO_2. Part 2, Appl. Catal. B-Environ. 126 (2012) 215–224.
[19] R.S.G. Ferreira, P.G.P. de Oliveira, F.B. Noronha, Characterization and catalytic activity of Pd/V_2O_5/Al_2O_3 catalysts on benzene total oxidation, Appl. Catal. B-Environ. 50 (2004) 243–249.
[20] Z.F. He, Z.R. He, D. Wang, Q.F. Bo, T. Fan, Y. Jiang, Mo-modified Pd/Al_2O_3 catalysts for benzene catalytic combustion, J. Environ. Sci.-China 26 (2014) 1481–1487.
[21] Z.F. He, D. Wang, T. Liu, H.Y. Wang, Y. Jiang, Nb-modified Pd/Al_2O_3 catalysts for benzene catalytic combustion, Chem. J. Chin. Univ. 35 (2014) 92–97.
[22] Q. Niu, B. Li, X.L. Xu, X.J. Wang, Q. Yang, Y.Y. Jiang, Y.W. Chen, S.M. Zhu, S.B. Shen, Activity and sulfur resistance of CuO/SnO_2/PdO catalysts supported on gamma-Al_2O_3 for the catalytic combustion of benzene, RSC. Adv. 4 (2014) 51280–51285.
[23] M. Hosseini, M. Haghighi, D. Kahforoushan, M. Zarrabi, Sono-dispersion of ceria and palladium in preparation and characterization of Pd/Al_2O_3-clinoptilolite-CeO_2 nanocatalyst for treatment of polluted air via low temperature VOC oxidation, Process Saf. Environ. 106 (2017) 284–293.
[24] H.C. Liao, P.Y. Zuo, M.M. Liu, Study on the correlation between the surface active species of Pd/cordierite monolithic catalyst and its catalytic activity, Mater. Sci. Eng. B-Adv. 211 (2016) 45–52.
[25] S. Pitkaaho, T. Nevanpera, L. Matejova, S. Ojala, R.L. Keiski, Oxidation of dichloromethane over Pt, Pd, Rh, and V_2O_5 catalysts supported on Al_2O_3, Al_2O_3-TiO_2 and Al_2O_3-CeO_2, Appl. Catal. B-Environ. 138 (2013) 33–42.
[26] J.C. Rooke, T. Barakat, S. Siffert, B.L. Su, Total catalytic oxidation of toluene using Pd impregnated on hierarchically porous Nb_2O_5 and Ta_2O_5 supports, Catal. Today 192 (2012) 183–188.
[27] Y.F. Wang, C.B. Zhang, Y.B. Yu, R.L. Yue, H. He, Ordered mesoporous and bulk Co_3O_4 supported Pd catalysts for catalytic oxidation of o-xylene, Catal. Today 242 (2015) 294–299.
[28] Y.F. Wang, C.B. Zhang, F.D. Liu, H. He, Well-dispersed palladium supported on ordered mesoporous Co_3O_4 for catalytic oxidation of o-xylene, Appl. Catal. B-Environ. 142 (2013) 72–79.
[29] S.H. Xie, Y.X. Liu, J.G. Deng, X.T. Zhao, J. Yang, K.F. Zhang, Z. Han, H. Arandiyan, H.X. Dai, Effect of transition metal doping on the catalytic performance of Au-Pd/3DOM Mn_2O_3 for the oxidation of methane and o-xylene, Appl. Catal. B-Environ. 206 (2017) 221–232.
[30] Y. Wang, H. Arandiyan, J. Scott, A. Bagheri, H.X. Dai, R. Amal, Recent advances in ordered meso/macroporous metal oxides for heterogeneous catalysis: a review, J. Mater. Chem. A 5 (2017) 8825–8846.
[31] S.H. Xie, J.G. Deng, Y.X. Liu, Z.H. Zhang, H.G. Yang, Y. Jiang, H. Arandiyan, H.X. Dai, C.T. Au, Excellent catalytic performance, thermal stability, and water resistance of 3DOM Mn_2O_3-supported Au-Pd alloy nanoparticles for the complete oxidation of toluene, Appl. Catal. A-Gen. 507 (2015) 82–90.
[32] F.J. Liu, S.F. Zuo, C. Wang, J.T. Li, F.S. Xiao, C.Z. Qi, Pd/transition metal oxides functionalized ZSM-5 single crystals with b-axis aligned mesopores: efficient and long-lived catalysts for benzene combustion, Appl. Catal. B-Environ. 148 (2014) 106–113.
[33] L. Yue, C. He, X.Y. Zhang, P. Li, Z. Wang, H.L. Wang, Z.P. Hao, Catalytic behavior and reaction routes of MEK oxidation over Pd/ZSM-5 and Pd-Ce/ZSM-5 catalysts, J. Hazard. Mater. 244 (2013) 613–620.
[34] C. He, J.J. Li, P. Li, J. Cheng, Z.P. Hao, Z.P. Xu, Comprehensive investigation of Pd/ZSM-5/MCM-48 composite catalysts with enhanced activity and stability for benzene oxidation, Appl. Catal. B-Environ. 96 (2010) 466–475.
[35] Z.K. Zhang, L.Y. Xu, Z.L. Wang, Y.J. Xu, Y.F. Chen, Pd/H beta-zeolite catalysts for catalytic combustion of toluene: effect of SiO_2/Al_2O_3 ratio, J. Nat. Gas Chem. 19 (2010) 417–421.
[36] M. Jablonska, A. Krol, E. Kukulska-Zajac, K. Tarach, V. Girman, L. Chmielarz, K. Gora-Marek, Zeolites Y modified with palladium as effective catalysts for low-temperature methanol incineration, Appl. Catal. B-Environ. 166 (2015) 353–365.
[37] S.F. Zuo, X.J. Sun, N.N. Lv, C.Z. Qi, Rare Earth-Modified Kaolin/NaY-Supported Pd-Pt Bimetallic Catalyst for the Catalytic Combustion of Benzene, ACS Appl. Mater. Interfaces 6 (2014) 11988–11996.
[38] W.X. Tang, Y.Z. Deng, Y.F. Chen, Promoting effect of acid treatment on Pd-Ni/SBA-15 catalyst for complete oxidation of gaseous benzene, Catal. Commun. 89 (2017) 86–90.
[39] C. Song, M. Chen, C.A. Ma, X.M. Zheng, Pd-Mn/stainless steel wire mesh catalyst for catalytic oxidation of toluene, acetone and ethyl acetate, Chin. J. Chem. 27 (2009) 1903–1906.
[40] M. Chen, Y. Ma, C. Song, T. Zhang, X.M. Zheng, Preparation and performance of Ce-Pt-Pd/stainless steel wire meshes catalyst, Chin. J Catal. 30 (2009) 649–653.
[41] S. Morales-Torres, A.F. Perez-Cadenas, F. Kapteijn, F. Carrasco-Marin, F.J. Maldonado-Hodar, J.A. Moulijn, Palladium and platinum catalysts supported on carbon nanofiber coated monoliths for low-temperature combustion of BTX, Appl. Catal. B-Environ. 89 (2009) 411–419.
[42] B.S. Balzhinimaev, E.A. Paukshtis, S.V. Vanag, A.P. Suknev, A.N. Zagoruiko, Glass-fiber catalysts: novel oxidation catalysts, catalytic technologies for environmental protection, Catal. Today 151 (2010) 195–199.
[43] S.F. Zuo, Y.J. Du, F.J. Liu, D. Han, C.Z. Qi, Influence of ceria promoter on shell-powder-supported Pd catalyst for the complete oxidation of benzene, Appl. Catal A-Gen. 451 (2013) 65–70.
[44] E. Reichelt, M.P. Heddrich, M. Jahn, A. Michaelis, Fiber based structured materials for catalytic applications, Appl. Catal. A-Gen. 476 (2014) 78–90.
[45] P. Petrova, T. Tabakova, G. Munteanu, R. Zanella, M. Tsvetkov, L. Ilieva, Gold catalysts on Co-doped ceria for complete benzene oxidation: relationship between reducibility and catalytic activity, Catal. Commun. 36 (2013) 84–88.
[46] Y.B. Li, C.B. Zhang, J.Z. Ma, M. Chen, H. Deng, H. He, High temperature reduction dramatically promotes Pd/TiO_2 catalyst for ambient formaldehyde oxidation, Appl. Catal. B-Environ. 217 (2017) 560–569.
[47] A. Aranzabal, J.A. Gonzalez-Marcos, J.L. Ayastuy, J.R. Gonzalez-Velasco, Kinetics of Pd/alumina catalysed 1,2-dichloroethane gas-phase oxidation, Chem. Eng. Sci. 61 (2006) 3564–3576.
[48] K. Okumura, T. Kobayashi, H. Tanaka, M. Niwa, Toluene combustion over palladium supported on various metal oxide supports, Appl. Catal. B-Environ. 44 (2003) 325–331.
[49] K. Okumura, S. Matsumoto, N. Nishiaki, M. Niwa, Support effect of zeolite on the methane combustion activity of palladium, Appl. Catal. B-Environ. 40 (2003) 151–159.
[50] X.Y. Wang, Y. Liu, T.H. Zhang, Y.J. Luo, Z.X. Lan, K. Zhang, J.C. Zuo, L.L. Jiang, R.H. Wang, Geometrical-site-dependent catalytic activity of ordered mesoporous Co-based spinel for benzene oxidation: in situ drifts study coupled with Raman and XAFS spectroscopy, ACS Catal. 7 (2017) 1626–1636.
[51] X.L. Liu, J.L. Zeng, W.B. Shi, J. Wang, T.Y. Zhu, Y.F. Chen, Catalytic oxidation of benzene over ruthenium-cobalt bimetallic catalysts and study of its mechanism, Catal. Sci. Technol. 7 (2017) 213–221.
[52] M.A. Bollinger, M.A. Vannice, A kinetic and DRIFTS study of low-temperature carbon monoxide oxidation over Au-TiO_2 catalysts, Appl. Catal. B-Environ. 8 (1996) 417–443.
[53] X. Chen, X. Chen, S.C. Cai, J. Chen, W.J. Xu, H.P. Jia, J. Chen, Catalytic combustion of toluene over mesoporous Cr_2O_3-supported platinum catalysts prepared by in situ pyrolysis of MOFs, Chem. Eng. J. 334 (2018) 768–779.
[54] Q.G. Dai, Q. Zhu, Y. Lou, X.Y. Wang, Role of Bronsted acid site during catalytic combustion of methane over PdO/ZSM-5: dominant or negligible? J. Catal. 357 (2018) 29–40.
[55] Y. Lou, J. Ma, W.D. Hu, Q.G. Dai, L. Wang, W.C. Zhan, Y.L. Guo, X.M. Cao, Y. Guo, P. Hu, G.Z. Lu, Low-temperature methane combustion over Pd/H-ZSM-5: active Pd sites with specific electronic properties modulated by acidic sites of H-ZSM-5, ACS Catal. 6 (2016) 8127–8139.
[56] J.G. Wang, C.J. Liu, Density functional theory study of methane activation over PdO/HZSM-5, J. Mol. Catal. A-Chem. 247 (2006) 199–205.
[57] K. Okumura, M. Niwa, Control of the dispersion of Pd through the interaction with acid sites of zeolite studied by EXAFS, Top. Catal. 18 (2002) 85–89.